

1 *Review*

2 **Chiroptical Sensing**

3 **Ani Ozcelik**¹, **Raquel Pereira-Cameselle**¹, **Natasa Poklar Ulrih**², **Ana G. Petrovic**^{3,*}, and
4 **José Lorenzo Alonso-Gómez**^{1,*}

5 ¹ Department of Organic Chemistry, University of Vigo, 36310, Spain; lorenzo@uvigo.es

6 ² Department of Food Science and Technology, Biotechnical Faculty, University of Ljubljana, Jamnikarjeva
7 101, 1000 Slovenia; natasa.poklar@bf.uni-lj.si

8 ³ Department of Life Sciences, New York Institute of Technology, New York, 10023, USA; apetro01@nyit.edu

9 * Correspondence: apetro01@nyit.edu (A.G.P.); lorenzo@uvigo.es (J.L.A.G.)

10 **Abstract:** Chiroptical responses have been an essential tool over the last decades for chemical
11 structural elucidation due to their exceptional sensitivity to geometry and intermolecular
12 interactions. In recent times, there has been an increasing interest for the search of more efficient
13 sensing by the rational design of tailored chiroptical systems. In this Review article, advances on
14 chiroptical systems towards their implementation in sensing applications are summarized.
15 Strategies to generate chiroptical responses are illustrated. Theoretical approaches to assist in the
16 design of these systems are discussed. Development of efficient chiroptical reporters in different
17 states of matter, essential for the implementation in sensing devices, is reviewed. In the last part,
18 remarkable examples of chiroptical sensing applications are highlighted.

19 **Keywords:** Chiroptical Systems; Theoretical Simulations, Chiral Design; Sensing Applications

20

21 **1. Introduction**

22 The concepts related to mirror-image symmetry have become a prominent topic as scientists
23 have made progress in structural determination of three-dimensional (3D) objects from both atomic
24 and molecular levels. Particularly, the presence or lack of mirror-image symmetry plays a crucial role
25 in shedding light on the origin of biological processes relevant to human life.[1] At different scales,
26 objects are said to be chiral when they do not coincide with their mirror image. Accordingly, achiral
27 objects are those possessing at least one improper axis i.e., a plane of symmetry or a center of
28 inversion (Figure 1).[2]

29

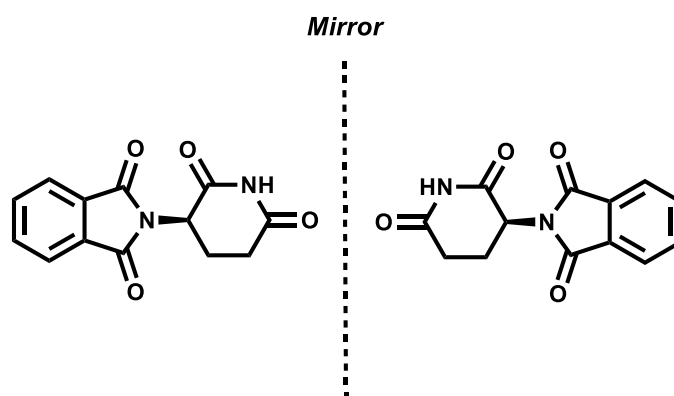


30

31

Figure1. Chiral (left) and achiral (right) macroscopic objects.

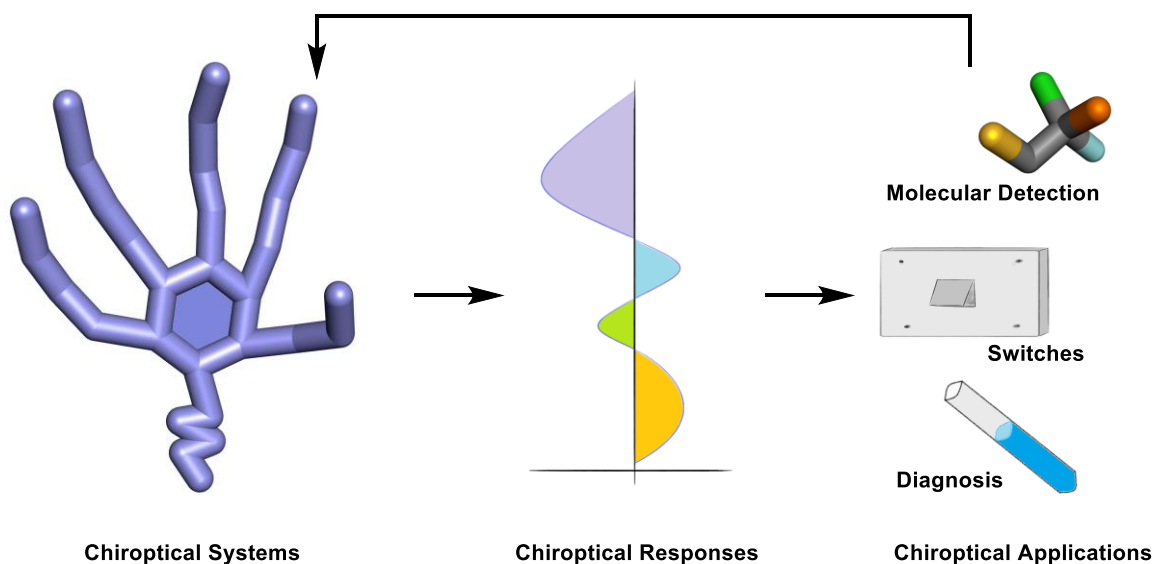
32 It was not until 1884 that the discovery of molecular chirality was achieved by Louis Pasteur
 33 when he observed left- and right-handed crystals of sodium ammonium tartrate tetrahydrate.[3]
 34 Today, it is known that a pair of opposite-handed-shapes are called enantiomers and their interaction
 35 with other chiral entities may give rise to distinct physiological and/or toxicological responses. As an
 36 example, thalidomide was used for the treatment of morning sickness in pregnancy in the late 50s
 37 and early 60s. While (*R*)-thalidomide was an effective analgesic, its enantiomer (*S*)-thalidomide had
 38 a teratogenic effect causing over 10,000 birth defects (Figure 2).[4]



39

40 **Figure 2.** (*R*)-Thalidomide (left) and (*S*)-Thalidomide (right).

41 Like molecules, light can also be chiral. In fact, the circularly polarized light-waves of opposite
 42 helicity, yet the same amplitude and phase, constitute the linearly polarized light. In this regard, the
 43 interaction of two enantiomeric molecules with the same helical wave may be different. The outcome
 44 of this distinction is known as circular dichroism (CD), a type of chiroptical response that can be used
 45 for several applications (Figure 3).[5]



46

47 **Figure 3.** General representation of the applicability of a chiroptical system.

48 The generation of chiroptical responses is very general, ranging from monodisperse to
 49 polydisperse systems, individual or collective chirality, of organic, organometallic, or inorganic
 50 nature, or even a combination of them. Also the applicability is wide, the absolute configuration

51 determination being the most frequently used after the discovery of chiroptical responses, but
52 nowadays also the conformational assignment of the responding systems, detection of chiral or
53 achiral molecules as well as the characterization of self-assemblies. Furthermore, the wavelength of
54 the induced chiroptical sensor readout is typically free of the interfering signals coming from the
55 sample under investigation. This spectral extension is advantageous in medical applications since
56 long exposure to light radiation can affect bimolecular samples.

57 The intent of this review is to provide the reader with a general overview of key aspects to take
58 into consideration when developing of a chiroptical system for sensing. It starts with an illustrative
59 description of the most commonly used strategies for the generation of chiroptical responses. Since
60 the signatures of the chiroptical responses are not trivial, different approaches for their prediction
61 have been developed, and here we summarize the most relevant ones. A desired application may
62 require of chiroptical systems to be in a particular state of matter, therefore, some examples herein
63 were classified concerning this aspect. Finally, some demonstrative examples of chiroptical sensing
64 are sketched on molecular detection, switches, and diagnosis.

65

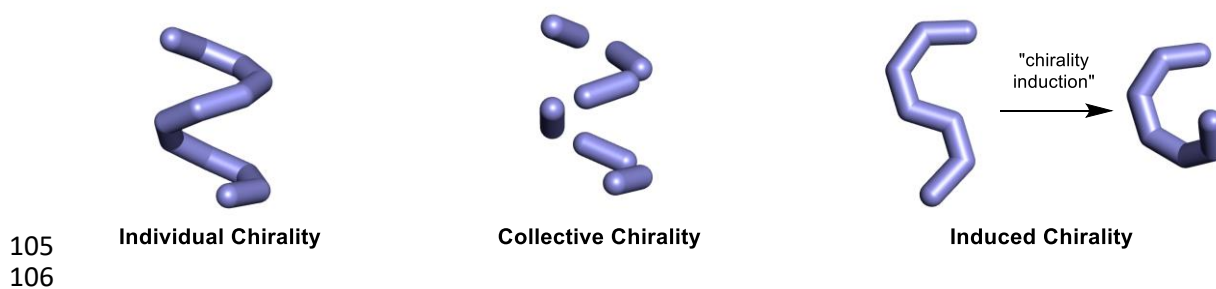
66 2. Strategies for the Generation of Chiroptical Responses

67 The rise of chiroptical methods, the key spectroscopic means of probing and reporting the
68 presence of chiral motive(s) within the molecular framework, came as a result of coinciding advances
69 in instrumentation as well as computer technology and algorithms that allow implementation of *ab*
70 *initio* theoretical simulations. In a timely manner, scientific community has made notable advances
71 in intelligent design of chiral systems capable of manifesting chirality in different ways: by selecting
72 chromophore providing chiral signals in specific spectral region or by fine-tuning the chiroptical
73 response via methodical selection of the preferred symmetry/geometry of the system in a given
74 media.

75 Historically, synthesis and isolation of chiral molecules has routinely incorporated
76 measurements of optical rotation (OR) at single sodium-D-line wavelength (589 nm) and electronic
77 CD (ECD) spectral signature. To achieve a reliable stereochemical structural elucidation, nowadays,
78 a simultaneous use of more than one chiroptical method is strongly encouraged: ORD, ECD, VCD,
79 and Raman optical activity (ROA).[6,7]

80 Different chiroptical methods probe chiral systems under variable conditions and with different
81 forms of energy, hence accessing different unique sensitivities to different structural features.
82 Specifically, UV-Vis linearly polarized light is used in the case of ORD, while circularly polarized
83 light in the case of ECD. VCD extends the functionality of ECD to the mid-infrared regime where
84 normal mode vibrational transitions are observed. Like VCD, ROA is a form of vibrational optical
85 activity that is sensitive to chirality associated with all fundamental vibrational normal modes. ROA
86 measures a small difference in the intensity of vibrational Raman scattering from chiral molecules in
87 right- and left-circularly polarized incident light. It is considered as insightful probe of the structure
88 and behavior of biomolecules in aqueous solution.[8,9] As such, different methods require different
89 solvation environments, different concentrations, different consideration of solute-solute vs. solute-
90 solvent interactions, as well as intra vs. intermolecular interactions.

91 In general, merits and limitations of a given chiroptical method can be identified when multiple
 92 methods are applied simultaneously to cross-examine a given stereochemical structural objective. As
 93 mentioned earlier, while OR at 589 nm is routinely reported, for structural elucidation it is advisable
 94 to consider the overall ORD pattern that extends over multiple wavelengths. While ECD requires a
 95 UV-Vis chromophore in order to produce a chiroptical response, in the case of VCD each 3N-6 normal
 96 mode vibrations have potential to serve as a chirality probe of N-atomic molecule. VCD typically
 97 access multiple well-define bands, yet it is less sensitive than ECD as reflected in the need for higher
 98 concentrations and 3-5 orders of magnitude lower intensity of the CD response.[10] Chiroptical
 99 response depends on the spatial orientation of chromophoric groups, moieties near the stereogenic
 100 centers and consequently on the overall molecular flexibility. Nonetheless, VCD is highly
 101 conformational sensitive, which is why in the case of flexible molecules it can be occasionally
 102 hindered by conformational averaging that leads to attenuation of the bands.[9] To reiterate, the best
 103 practice is to resort to multiple chiroptical method in order to increase the confidence level of the
 104 assignment. [6]

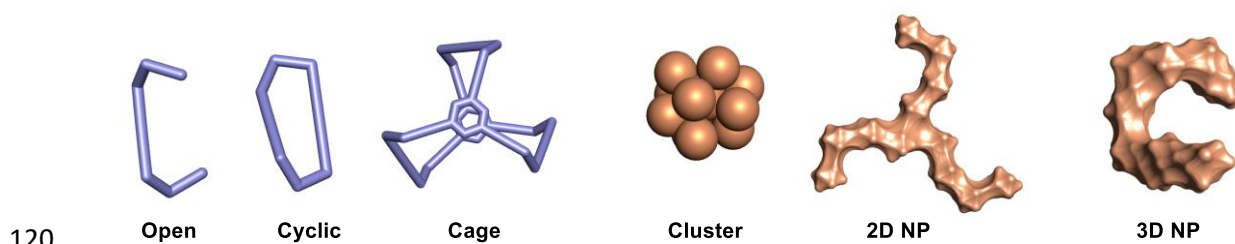


107 **Figure 4.** Different strategies to chiroptical systems.

108 Chirality can be manifested in many different ways, in this section we group chiroptical systems
 109 originating from three different strategies: **Individual**, **Collective**, and **Induced Chirality** (Figure 4).
 110 Other approaches to render chiroptical systems such as integrated photonics,[11] are not in the scope
 111 of this review.

112 2.1. Individual Chirality

113 In this section we want to call the attention over systems that independently present chirality.
 114 Considering individually chiral systems one may identify them as being from molecular or
 115 nanoparticle nature (Figure 5). Very often the open molecular systems are monodisperse,[12]
 116 however, there are several examples of open polydisperse oligomers presenting chiroptical
 117 responses.[13] On the search for specific molecular recognition sites and restriction of the
 118 conformational space, several cases have been developed on cyclic[14] and cage-like organic[15] and
 119 organometallic systems.[16]

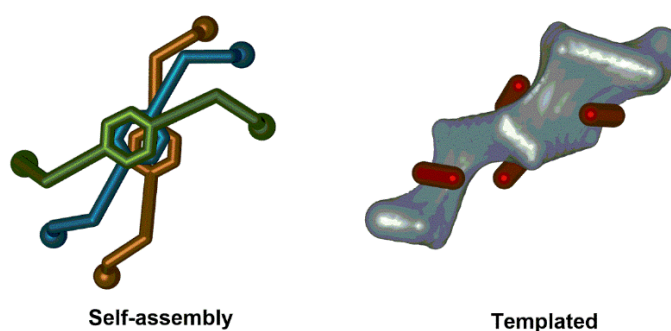


121 **Figure 5.** Different examples of systems presenting individual chirality.

122 On the other hand, a tremendous expansion in the last years has been realized in the
123 development of intrinsically chiral metal nanoparticles. While for clusters, the system can be
124 monodisperse, larger nanoparticles are typically polydisperse and can be classified as 2D chiral
125 nanoparticles, where the chirality comes from the nanoparticle lying onto a surface, or 3D chiral
126 nanoparticles.[17]

127 2.2. Collective Chirality

128 Collective chirality is referred to the global asymmetry featured by 3D complex
129 nanoarchitectures. The asymmetric organization of chiral or achiral entities mainly stems from
130 specific weak interactions through space rather than covalent bonding. This reality can be realized
131 by self-assembly or template strategies (Figure 6).



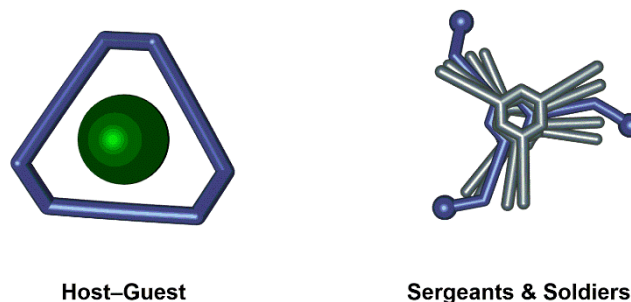
132

133 **Figure 6.** Representation of self-assembly and template-guided self-assembly processes to reach
134 collective chirality in 3D nanoarchitectures.

135 To reach collective behavior in a variety of complex nanostructures with chiral morphology,
136 bottom-up approach has been utilized for many decades. As an example, gel formation of a chiral
137 azobenzene via π - π stacking was attributed to be mainly responsible for the observed chiroptical
138 responses since the isolated molecular system employed is practically CD silent.[18] On the other
139 hand, template-guided self-assembly involves the interaction between entities and templates to tackle
140 challenges in precise control of self-assembly at nanometer scale. For instance, well-defined
141 arrangement of plasmonic nanoparticles can be achieved when inorganic silica helices are used as a
142 chiral template. This complex architecture features remarkable chiroptical responses as a result of the
143 helical arrangement of the metal nanoparticles.[19]

144 2.3. Induced Chirality

145 The expression of chirality in achiral molecules and molecular assemblies is known as induced
146 chirality. Typically, chiral induction is achieved when units comprising the system are arranged in
147 an asymmetric or helical manner, even though constituents of the system are achiral. From
148 mechanistic perspective, chiral induction at the supramolecular level can be generated via host-guest
149 complexation or by the formation of vividly termed sergeant-and-soldiers (Figure 7). Chiral induction
150 and tunable helicity control in oligomers, host-guest complexes, and supramolecular assemblies is a
151 desirable goal in view of appealing applications in material science. Below we present few selected
152 systems that demonstrate the induction and amplification of supramolecular chirality from achiral
153 molecules.



154

Host-Guest

Sergeants & Soldiers

155 **Figure 7.** Representation of host-guest and sergeants and soldiers strategies for chiral induction.

156 The folding of biopolymers into compact architectures capable of encapsulating ligands has
 157 inspired chemists to design artificial receptors based on helically folded oligomers possessing a
 158 hollow cavity. In many cases, oligomeric-foldamers have demonstrated propensity to strongly
 159 express homo-chirality by providing confined environments suited to recognizing chiral guests with
 160 high enantioselectivity. The binding of chiral guests can lead to dynamically responsive helical
 161 chirality of an oligomeric-foldamer which serves as the host.[20] For instance, the addition of chiral
 162 monoterpenes results in induction, increase and eventual saturation of the CD signal for achiral
 163 oligomeric phenylene ethynylene.[21] Further developments in designing foldamers susceptible to
 164 helical-bias have included higher degree of modularity of such receptors.[22] Another type of
 165 induced chirality within host-guest complexes occurs when chirality is transferred from chiral non-
 166 chromophoric systems to chromophoric groups that adopt chirality and serve as chiral sensors. A class
 167 of achiral molecules susceptible to such chiral imprinting are metalated bis-porphyrin tweezers. A
 168 wide array of dimeric porphyrin hosts has been developed and applied towards the absolute
 169 configuration (AC) assignment of several classes of mostly bifunctional chiral compounds such as
 170 diamines, amino alcohols, or amino acids.[23,24] Upon formation of 1:1 host-guest complex through
 171 bidentate metal coordination, chirality is transferred from the guest to the host with the effect of
 172 inducing a preferential chiral twist in the porphyrin-porphyrin arrangement. The sign of the Soret
 173 CD couplet is related to, and diagnostic of the AC of the guest. On the other hand, diverse achiral
 174 guests such as nonchromophoric[16] or organometallic sandwich[25] can be detected due to chiral
 175 induction through inclusion complex formation with helical molecular cages.

176 Sergeant-and-soldier induction mechanism involves a small amount of chiral material (sergeant)
 177 that enforces a chiral structure on assembly composed predominantly of achiral molecules (soldiers)
 178 as dictated by the chirality of the sergeant. To date, numerous systems exhibiting induced chirality
 179 have been reported using this principle.[26,27] One example of sergeant-and-soldier phenomena is
 180 the induced helicity of isotactic-rich poly(2-vinylpyridine) by means of its hydrogen-bonding with
 181 chiral hexahydromandelic acid. The mirror imaging of the CD spectra suggests the formation of right-
 182 and left-handed helical chains of the achiral polymer through complexation with the chiral guest.[28]
 183 Poly(phenylacetylene)s have also shown to present distinct chiroptical responses associated with
 184 their helicity. These systems can remarkably switch conformation upon complexation with different
 185 guests.[29]

186

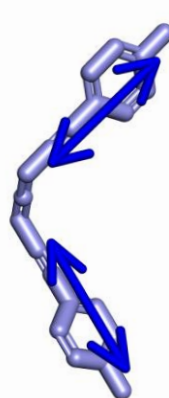
187 3. Approaches for the Prediction of Chiroptical Responses

188 The prediction of the chiroptical responses is not trivial, and therefore different methodologies
 189 have been developed for their prediction. *Ab initio* calculations have been extensively used for small
 190 and medium sized molecular systems, not far above 1000 heavy atoms. The specific level of theory
 191 may be chosen not only considering the chiroptical response under evaluation but also the nature of

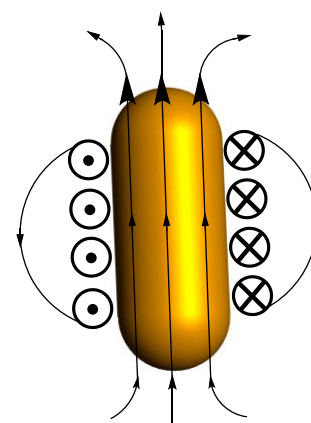
192 the chiroptical system. A much more intuitive method for the prediction of chiroptical responses is
193 the exciton chirality (EC) method, this method is reliable when the chromophores mainly responsible
194 for the response in the system are independent, no direct conjugation between them, and may interact
195 to each other through space. While EC has been extensively used for interpretation of ECD
196 signals,[30] more recently it has also been implemented in the analysis of VCD spectral profiles.[31]
197 Nonetheless, an extension of the EC concepts to VCD has to be applied and interpreted with great
198 care to prevent possible erroneous predictions.[32]



199 **ab initio**



200 **Exciton Chirality**



201 **Classical Electromagnetism**

202

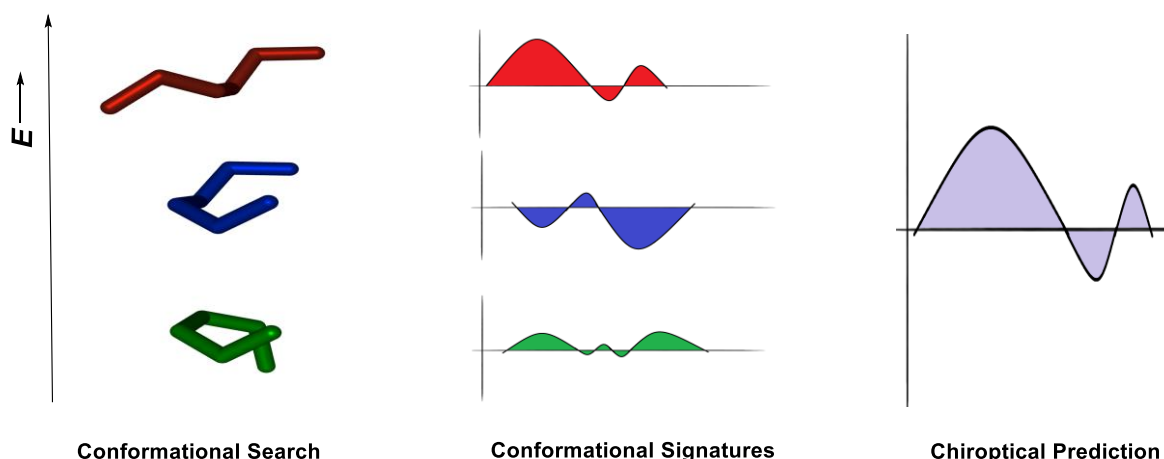
203

Figure 8. Different approaches for chiroptical prediction.

204 The prediction of the chiroptical responses via EC method has been typically applied by the
205 summation of the pairwise interactions among all chromophores. Specifically, for systems with high
206 symmetry, a chiroptical symmetry analysis may help on the design of chiroptical systems. On the
other hand, for systems presenting surface plasmon resonance, methodologies based on classical
electromagnetism are often used (Figure 8).

207 3.1. *Ab Initio*

208 The exponential growth of computational power has been the key driving force that revolutionized
209 the way chemists approach the stereochemical structural elucidation without the need for any
210 additional chiral reagents, chemical derivatization or reference system.[33] As such, simulations
211 related to identifying stable geometries and predicting corresponding chiroptical responses from first
212 principles (*ab initio*) have become indispensable tool in investigating chiral molecular systems. A
213 large number of research studies have demonstrated that molecular chiroptical properties can be
214 computed reliably, starting from first principles quantum theory, particularly Density Functional
215 Theory (DFT) (Figure 9).



216

Conformational Search

Conformational Signatures

Chiroptical Prediction

217

Figure 9. Necessary steps for the chiroptical prediction.

218 A number of recent review articles, for instance references,[8,34–38] document the progress
 219 made in the computational chiroptics. Simulations are used to predict and visualize stable
 220 conformations, to assign absolute configurations, to simulate and analyze chiroptical data, as well as
 221 to provide a basis for understanding their origin. Additionally, simulations can provide supporting
 222 evidence and insight into the origin of chiral induction phenomena. On the other side of the coin,
 223 since molecular modeling always yields data, one needs to be mindful not to treat molecular
 224 modeling as a black-box tool or take the quality of simulated data for granted.[8,10,38] In this section,
 225 we discuss key steps with a few examples aimed at highlighting the most critical aspects of the ab
 226 initio protocol towards chiroptical structural elucidation. As routine to computational chemistry, ab
 227 initio based chiroptical predictions begin with building virtual model(s) and for each model
 228 conducting conformational survey aiming to identify prevailing molecular geometries. In this initial
 229 step, empirical data from NMR spectroscopy and X-ray crystallography could yield the relative
 230 configuration (RC) of selected stereogenic centers which can significantly reduce the number of
 231 necessary virtual models. An illustrative example of valuable a-priory RC determination is the study
 232 of marine natural product (+)-bistramide C, which is endowed with 10 stereogenic centers.[39]
 233 Specifically, NMR based study has reduced the candidate pool of 1024 possible stereoisomers, to only
 234 16 diastereomers needed for ECD theoretical consideration. In the absence of RC data, for system
 235 with n elements of chirality, one must consider all $2n-1$ diastereomers, mindful that enantiomeric
 236 forms provide mirror image chiroptical responses.

237 The most common approach to identify the local minima is to initiate the survey of potential
 238 energy surface (PES) by resorting to molecular mechanics (MM) based molecular dynamics (MD) or
 239 Monte Carlo (MC) algorithms with a well mindful selection of parametrized force field based on
 240 atom-types and moieties (e.g. MMFFs, OPLS3, AMBER, etc.). It is of critical importance that
 241 conformational survey is conducted in a comprehensive manner in order to avoid any carryover
 242 errors from this initial step that have negative consequences on the final chiroptical results and are
 243 challenging to track-back. Even if the conformer is not highly populated, it could intrinsically provide
 244 a strong chiroptical response and, as such, have influence on the overall predicted spectral signature.
 245 Therefore, the use of multiple algorithms and possibly applicable force fields are advisable[8,37,38]
 246 in order to properly explore variation in all rotatable bonds and overcome energy barriers associated
 247 with ring-puckering modes.

248 The stable MM-identified geometries within ~10-20 kcal/mol energy window[40], depending on
 249 the intrinsic degrees of freedom, are subsequently fully optimized under appropriate quantum
 250 mechanical levels of theory. For larger molecular systems, it is not uncommon to firstly apply semi-
 251 empirical AM1 or PM3 methods, followed by full geometry optimization at higher ab initio level of
 252 theory. DFT which encompasses a large variety of different levels of approximation, levels of theory,
 253 has been benchmarked as a standard computational method, yielding the best average performance

254 for energy minimization and chiroptical predictions. Contrary to colloquial statement “one size fits
255 all”, in choosing the appropriate DFT-based level of theory, there is no classification of molecular
256 system by size or atom type that allows for single universal reliable approach. Every simulations
257 method is prone to error.[41] Therefore, one should resort to exploring different combinations of DFT
258 functionals and basis sets in search of consistencies in Boltzmann populations of stable conformations
259 as well as, at later stage, corresponding chiroptical responses. Simulation results that are more
260 consistent among each other and, most importantly, that more closely correlate with the experimental
261 data are considered as delivering a higher confidence level results. Identification of true PES minima
262 resulting from the full geometry optimization is verified by the absence of negative vibrational
263 frequencies at the same level of theory.

264 Two suggested families of functionals that can be explored are hybrid and range-separated ones.
265 Popular hybrid functional with increasing amounts of “exact” HF exchange integral are B3LYP (20%
266 HF), PBE0 (25%), M06 (27%), BH&HLYP (50%), and M06-2X (54%). Range-separated functionals such
267 as Coulomb-attenuated CAM-B3LYP and ω B97X functionals often outperform the hybrid ones in
268 ECD predictions and, hence, are considered standard. One instructive illustrative example can be
269 found in references [38,42]. It is important to emphasize that relative Gibbs free energies, dipole and
270 rotational strength can be very sensitive to the choice of functional. Literature provides several
271 cautionary tales of studies which demonstrate that popularly used B3LYP is not necessarily the most
272 accurate functional for predicting structures and energies of standard organic molecules, especially
273 when noncovalent interactions come into play.[8,38,42–45]

274 While 6-31G* can be used as the most fundamental basis set to obtain initial simulation-based
275 insight, double-zeta- ζ or triple- ζ as well as augmented basis sets (aug-TZVP, aug-cc-pVDZ) as well
276 as those with polarization functions (6-311++G(2d,2p)) are recommended as capable of producing
277 quality chiroptical outcomes. If ionic species are involved, diffuse functions must be included within
278 the basis set selection. Los Alamos National Laboratory 2 Double-Zeta, LANL2DZ basis set[21] is
279 extensively tested effective core potential to model metal atoms.[22] Benchmark investigation
280 demonstrates that CAM-B3LYP with the aug-cc-pVDZ basis set can be a useful method considering
281 both accuracy and reasonable computational time to predict the Boltzmann average optical rotation
282 that matches the experimental, and thereby the absolute configuration of chiral molecules.[46] An
283 illustrative case for which both geometry optimization and TDDFT calculation of chiroptical property
284 can be highly sensitive to the used basis set is the ORD-based investigation of isocytosaxone.[47]

285 While functional and basis set should be varied and explored for consistency, the solvent model
286 should be accounted to match the media used for experimental chiroptical measurements. Solvent
287 may affect the relative stability of conformers, especially with propensities for non-bonding
288 interactions. In most cases continuum solvent models such as conductor like screening model
289 COSMO and polarizable continuum model PCM are satisfactory. According to few case-studies, the
290 reliability of PCM predictions of solvent effects on optical rotations is dependent on the solvent
291 chosen.[48] If spectral predictions are not optimal and verifying level of theory do not improve the
292 level of correlation, one may choose to resort to explicit solvent to account for specific solute-solvent
293 and solute-solute (dimer, trimer) interactions. For examples of such a procedure, we refer the
294 interested reader to the literature. [49–53]

295 Besides the choice of functional and basis set, vibrational effects can play notable role in the
296 simulated chiroptical response, especially in the case of ORD and ECD. Predicted electronic
297 chiroptical data in which molecule’s environment and inclusion of vibrational effects have been taken
298 into consideration have generally improved agreement with experimental data. One illustrative
299 example is the ORD-based structural elucidation of (R)-methyloxirane by means of a novel
300 computational protocol, involving MD trajectory, able to take into account vibrational averaging and
301 solvent effects, leading for the first time to a quantitative agreement (both sign and absolute value)
302 between computed and experimental OR values at several frequencies.[54] This research area will
303 remain highly active as new computational methods are being developed.

304 Chiroptical properties are subsequently computed from first principles and Boltzmann averaged
305 based on predicted Gibbs free energies if more than one stable structures ($\Delta E \leq 1$ kcal) are identified.
306 The variability of ab initio predicted chiroptical signals depending on conformer, underscores the
307 importance of thorough conformational exploration and geometry optimization as a fundamental and
308 one of the most important step in carrying out AC assignment.[47] In general, the weaker the
309 experimental chiroptical response and/or the more conformationally flexible the molecular system
310 under study, the more likely will be its dependence on the calculation method, including functional,
311 basis set, and solvation model. As previously mentioned, TDDFT has been established to be main
312 state-of-the-art technique to obtain accurate numerical results for chiroptical predictions. In addition,
313 methods that have been used to provide trustworthy chiroptical spectroscopic response are time
314 dependent HF (TDHF)[15] and more computationally demanding coupled cluster (CC) method. For
315 larger systems with up to 1000 atoms, simplified TDDFT (sTDDFT) method has been recently
316 introduced as good combination between computational cost and satisfactory accuracy for ECD
317 prediction.[55]

318 Typically, when ECD and VCD spectra are simulated, the computed stick spectra corresponding
319 to vertical electronic and vibrational transitions are broadened with Gaussian and Lorentzian
320 functions, respectively. ECD spectra often require a global shift of the excitations, because of the
321 tendency of TDDFT to underestimate excitation energies.[8,56] Therefore, the excitation energies are
322 typically shifted by +0.2eV to +0.45eV. On the other hand, due to variation method nature of the
323 approach of calculating VCD signals, vibrational energies are typically overestimated and need to be
324 downshifted by factors recommended depending on the given basis set level of theory.

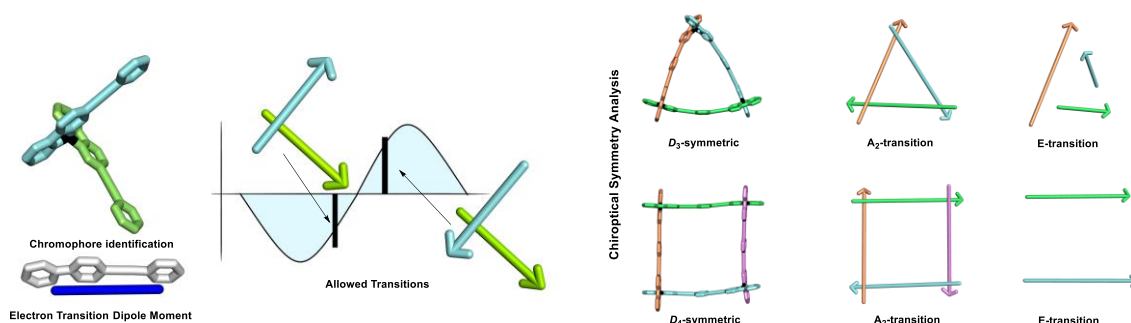
325 It might appear that ab initio predictions of multiple chiroptical spectroscopic methods are likely
326 to give redundant structural information. However, at the very least, simulations of multiple
327 chiroptical responses serve as independent verifications of molecular structures. In general, the
328 weaker the computed chiroptical spectrum, the stronger the dependence on the level of theory
329 (functional, basis set and solvation model selection). When a given chiroptical spectroscopic method
330 gives ambiguous results, the use of more than one chiroptical spectroscopic method may provide
331 missing information and increase the overall confidence level of the stereochemical assignment.

332 It is worth mentioning that in the past decade it has been brought to light that traditional solely
333 qualitative correlation between experimental and ab initio predicted spectral profiles can provide
334 limiting and even misleading analyses as such approach overlooks the valuable stereochemical
335 information embedded within the corresponding electronic absorption (EA) as well as electronic
336 dissymmetry factor (EDF) spectra. Therefore, one of the recent trends pioneered by Polavarapu et al.
337 is to correlate theoretical vs. experimental ECD, EA and EDF spectra in order to enhance applicability
338 as well as increase confidence level of stereochemical structural elucidations via electronically-based
339 chiroptical spectroscopy. As such, quantitative correlations between experimental and theoretical
340 electronic signatures represent the suggested overall ab initio protocol. Algorithms have been
341 implemented in general-purpose programs such as CDSpecTech which helps generate, cross-
342 correlate and quantitatively score the degree of overall between theoretical and experimental EA,
343 ECD, and EDF spectra. We refer readers to further literature for recent case studies which
344 demonstrate the scope of applicability and benefits of applying novel quantitative ECD approach
345 towards reliable stereochemical elucidations.[57–59]

346 3.2. Exciton Chirality

347 When two equivalent chromophores are present in the same system, the apriory degenerated
348 associated electronic transitions, may split into two nondegenerated in-phase and out-of-phase
349 transitions. Figure 10 shows the electron transition dipole moment (ETDM) associated with a
350 chromophore and the two possible associated transitions for a systems incorporating two of them.
351 Additionally, if the two chromophores have a mutual chiral arrangement, the specific chiroptical
352 signature can be easily associated with such chiral arrangement.[60] Particularly, if the Cotton effect of

353 lower energy is positive and the other negative, the torsion angle between the two associated ETDMs
 354 is positive, the opposite is true for the contrary. This simple relation between the CD response and
 355 the geometry of the chiroptical system has been extensively used not only for the relative and
 356 absolute configuration of complex systems, but also for the detection of molecular systems.[61]



357

358 **Figure 10.** Example of exciton chirality and chiroptical symmetry analysis.

359 For systems presenting more than two independent chromophores, the chiroptical responses
 360 may be determined by the summation of the chiroptical responses originated for pairwise coupling
 361 between all chromophores. However, if the system presents higher symmetry, a chiroptical
 362 symmetry analysis can be employed as alternative.[62] The chiroptical symmetry analysis of
 363 trianglimines has been recently performed as a case study.[63]

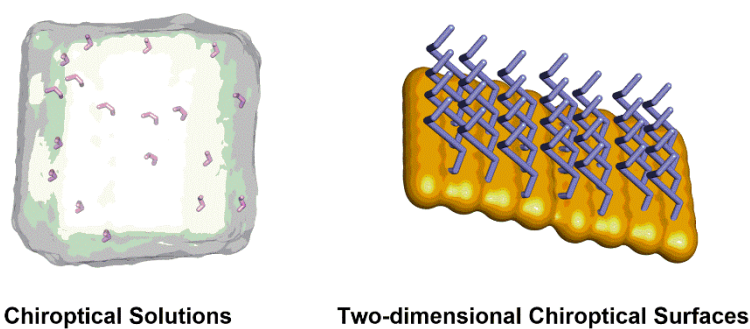
364 3.3. Classical Electromagnetism

365 As for the case of large molecules, more than 100 heavy atoms, the prediction of the chiroptical
 366 responses of metal nanoparticles is not typically affordable using ab initio for most of the cases. This
 367 field has greatly developed recently and is the subject of other reviews,[64] therefore we refer the
 368 reader to them for a more specific reading on the topic.

369

370 4. Chiroptical Systems on Different States of Matter

371 There is a vast amount of chiroptical responding systems, with fewer of them employed in
 372 chiroptical applications. Among the requirements the applicability of chiroptical systems, one needs
 373 to take into account the state of matter required for a specific application.



374

375 **Figure 11.** Illustration of chiroptical systems in different states of matter.

376 Therefore, we want to draw the attention of the reader in this section to chiroptical samples that
 377 are in solution and two-dimensional surfaces (Figure 11).

378 4.1. Chiroptical Solutions

379 Chiroptical solutions are by far the most abundant among chiroptical systems. The g-factor, the
380 ratio between circular dichroism and absorption, is typically used as a measure of the chiroptical
381 power. Therefore, this parameter is often used to evaluate the chiroptical responses. The highest
382 reported for purely organic molecules are 0.05 for polyaromatic systems[65] 0.01 for alleno-[66]and
383 spiro-acetylenic[14] oligomers, and 0.06 for protein complexes.[67] On the other hand, colloidal small
384 metal nanoparticles present typically values below 0.001[68] while fluid suspensions of nanorods
385 may reach a g-factor c.a. 0.022.[69]

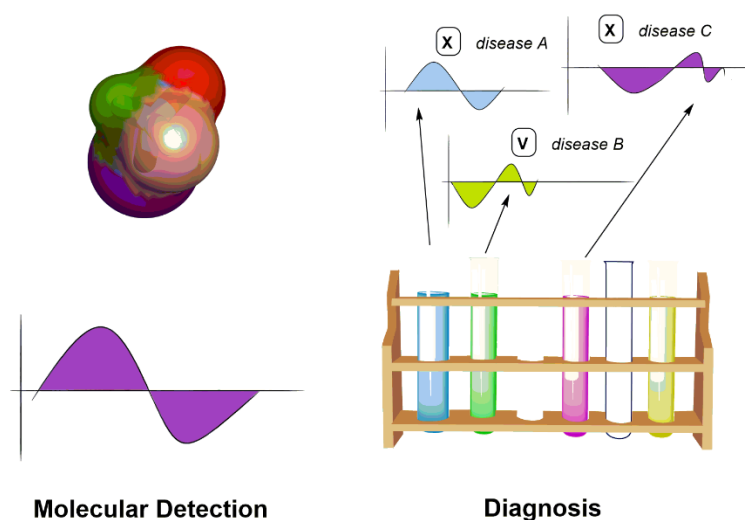
386 4.2. Two-dimensional (2D) Chiroptical Surfaces

387 Chiroptical methods have been extensively used for the structural characterization of chiral
388 systems and complexes due to their high sensitivity as mentioned above. To expand their
389 applicability in today's world, the development of 2D surfaces with tailored chiroptical properties is
390 essential. Such complex systems are described as those nanostructures lacking mirror-image
391 symmetry in solid state. Among other strategies, the inherent chirality of either small or large
392 molecules could be transferred to achiral metal substrates upon self-assembly. Regarding the former
393 case, Wälti and co-workers conducted a conformational study on monolayers of synthetic peptide by
394 means of CD spectroscopy.[70] On the other hand, unlike large molecular systems, the exploration of
395 chiroptical responses featured by single monolayers of small molecules might require more
396 sophisticated chiroptical methods. In this regard, the chiral 2D ordering of allenes on a metal surface
397 has been previously studied by scanning tunneling microscopy, however, the low stability hampered
398 the exploration of the chiroptical responses of the monolayer.[71] Recently, incorporation of
399 anchoring groups to the allenic moiety enabled the formation of device-compatible chiroptical
400 surfaces. Whereas the conventional CD spectroscopy measurements have yielded unambiguous
401 results, the chiroptical responses of these molecule-thin sheets have been addressed via second
402 harmonic generation spectroscopy on a custom-made transparent substrate.[72]

403

404 5. Chiroptical Sensing Applications

405 Chirality plays an essential role in life, providing unique functionalities to a wide range of
406 biomolecules, natural products, and drugs, which makes chiral sensing and analysis critically
407 important. The wider application of chiral sensing continues to be constrained by the involved chiral
408 signals being inherently weak. Despite the tremendous importance of chiral sensing, its application
409 remains very limited, as chiroptical signals are typically very weak, preventing important biological
410 and medical applications. In this session we will give an overview of some of the existing applications
411 of chiroptical sensing such as molecular detection, and diagnosis (Figure 12).



412

Molecular Detection**Diagnosis**

413

Figure 12. Representation of chiroptical applications.414 *5.1. Chiroptical Molecular Detection*

415 The future perspectives of chiroptical sensing require sensitivities beyond current limits,
 416 including (i) determination of protein structure in-situ, in solution, at surfaces, and within cells and
 417 membranes, (ii) chiral analysis of body fluids as a diagnostic tool in medicine; (iii) metabolomics e.g.
 418 coupling the chromatographic separation techniques with chiral identification of the components of
 419 complex mixtures, (iii) creating new standards for the pharmaceutical and chemical analysis
 420 industries; (v) measurement of single-molecule chirality. Chiral sensing processes in general consist
 421 of two processes, molecular sensing and signal transduction. If we more closely consider intelligent
 422 chiral sensors, inclusion of concepts on nanotechnology and nanomaterials becomes more important.
 423 There have been great advances in nanostructure fabrications and some of these efforts have
 424 successfully created novel, useful concepts such as the atomic switch, probe-fabrication of molecular
 425 arrays, and integrated circuit technology. In addition, various nanostructures have now become
 426 available such as carbon nanotubes and other nanotubes, nanosheets, nanoparticles, nanorods,
 427 nanowires, nanowhiskers, mesoporous silica, mesoporous carbon and other mesoporous materials,
 428 organic-inorganic nanohybrids and bio-related nanohybrids.[73]

429 In recent years, the research in the field of chiroptical sensing has been focused on metamaterial
 430 and plasmonic platforms for manipulating local fields to enhance the chiroptical signals.
 431 Metamaterials can enhance the chiroptical signals of various biomolecules whose optically active
 432 bends lie in the ultraviolet (UV), visible, and infrared (IR) frequencies.[64] The metamaterial platform
 433 includes the chiral and achiral types according to their structure. An advantage of using the chiral
 434 sensing platform is creating a strong optical chirality in the vicinity of chiral metamaterials. Chiral
 435 metasurfaces, in principle, allow unambiguous detection of large chiral molecules. The first use of
 436 metasurface which a single layer gammadion structure was used for detecting various proteins and
 437 the amino acid tryptophan.[74] The main mechanism is based on measuring the spectral shift in the
 438 far field spectrum due to the near field interactions between the chiral molecules and the metasurface.
 439 Similarly, the metal Shuriken metamaterial was applied for IgG. The same mechanism was later
 440 extended to different smaller chiral molecules.[75–78]

441 Chiral metamaterial platforms have limitation due to the strong CD signal generated by the
442 platform itself, which can contaminate the relatively weak molecular signal. To overcome the
443 limitations of the chiral metamaterial platform, achiral metamaterials have been introduced. The CD
444 response of a chiral molecule may be significantly boosted around the resonance frequency of a
445 plasmonic nanosphere, with a resultant CD is still in the millidegree range, but now extended to the
446 visible spectrum. This spectral extension is advantageous because long exposure to ultraviolet
447 radiation can affect bimolecular samples. However, plasmonic achiral structures do not allow a
448 univocal chiral detection because the sign of the CD spectrum is sensitive to the binding orientation
449 of the chiral molecule to the plasmonic nanoparticles.[79]

450 On the other hand, the constructions of nanosized supramolecular hosts via self-assembly of
451 molecular components has tremendous applications in many field of chemistry and technology,
452 material science and sensors development. The formed nanostructures are derived from multiple,
453 weak, and noncovalent interactions such as electrostatic and van der Waals forces or hydrophobic
454 effects, π - π stacking interactions, metal coordination, and hydrogen bonding. Capitalizing the
455 plurality of weak interaction pathways, molecules can self-assemble giving different nanostructure
456 motifs, such as tubes, rods, and sheets.[80] Porphyrins, metalporphyrins, and their assemblies afforded
457 a large number of nanomaterials featuring various electronic and structural characteristics, like rods,
458 rings, particles, sheets, wires, and tubes.[81] The presence of a cationic chiral functionality on the
459 porphyrin periphery results in the achievement of solid-state systems expressing elements of
460 supramolecular chirality. A tetraphenylporphyrin bearing an (L)-prolinium moiety at one of the
461 peripheral phenyl groups has a cationic chiral functionality steers the self-aggregation process
462 toward the formation of large porphyrin aggregates featuring high supramolecular chirality, as
463 evidenced by their CD spectra. This material shows high sensitivity to limonene.[82] In solution,
464 achiral diporphyrins have also been extensively used for the chiroptical detection of a large diversity
465 of chiral synthetic compounds and natural products.[24,49] Similarly, β -cyclodextrin is an ideal host
466 for forming supramolecular structure due to its well-defined hydrophobic inner cavity and
467 hydrophilic shell. β -cyclodextrin has the ability to selectively combine miscellaneous inorganic,
468 organic and biomolecules into its cavities to the formation of the host-guest inclusion complex. The
469 inherent chirality of this systems was used for the chiroptical detection of resveratrol.[50] Helical
470 organometallic[16] and purely organic cages[15,25] have been used for the chiroptical detection of
471 diverse molecular systems.

472 5.2 Chiroptical Diagnosis

473 Plasmonic nanoparticles (NPs) were proposed as materials with great potential for biomedical
474 applications, such as biosensing, drug delivery, or photothermal therapy.[51] In this section, we will
475 present a few cases of successful use of chiroptical sensors in diagnostics of different diseases.
476 Prostate-specific antigen (PSA) is a specific biomarker of prostate cancer and it is found in both
477 diseased and normal prostate cells. Tang developed a highly selective chiroptical detector of PSA
478 based on gold nanorod (Au NR) dimers assembly via complementary DNA fragments. The CD
479 signals were amplified by a silver shell deposition on the surface of the gold nanorod dimers. This
480 biosensor was postulated to serve as a versatile methodology for cancer biomarkers.[52]

481 The expansion of age-related neurodegenerative disorders associate with increased life
482 expectancy has emerged as a topic of fundamental importance in scientific research. Many of these
483 diseases, including Alzheimer's disease, Parkinson's disease, amyotrophic lateral sclerosis, and
484 transmissible spongiform encephalopathies, are characterised by the presence of amyloid deposits
485 made of misfolded proteins. Therefore, tools allowing the detection of specific forms of protein
486 aggregates are pivotal to improve the knowledge on fundamental aspects of these neurodegenerative
487 disorders. Golden nanorodes were successfully used to detect amyloides in Parkinson's and prion
488 diseases using plasmon chirality. The nanorods do not react with monomeric protein but are
489 absorbed onto helical protein fibrils. Chiral amyloid templates, therefore, induce a helical
490 arrangement of nanorodes, giving rise to intense optical activity at the plasmon resonance
491 wavelengths.[55]

492 Type 1 diabetes mellitus is characterized by a permanently elevated level of blood glucose and
493 altered levels of other biomarkers, and by changes in the conformation of blood plasma proteins and
494 other biomolecules associated with the pathogenesis of diabetes. However, the observation of these
495 structural changes by conventional Raman and infrared spectroscopy is limited. The chiroptical
496 spectroscopy, which is inherently sensitive to the 3D structure of chiral molecules and able to detect
497 any possible structural changes. Identification of spectral biomarkers for type 1 diabetes mellitus
498 using the combination of chiroptical and vibrational spectroscopy results suggest that chiroptical
499 spectroscopy gives more detailed information about the 3D structure of biomolecules and therefore,
500 might be a promising complement to conventional diagnostic methods.[83]

501 Most plasmonic sensors and systems to date have been rigid and passive. However, rendering
502 these dynamic structures opens new possibilities for applications. The dynamic plasmonic
503 nanoparticles developed by Jeong and co-worker can be used as mechanical sensors to selectively
504 probe the rheological properties of a fluid in situ at the nanoscale and in microscopic volumes. They
505 have fabricated chiral magneto-plasmonic nanocolloids that can be actuated by an external magnetic
506 field, which in turn allows for the direct and fast modulation of their distinct optical response. Such
507 noninvasive measurements by optical plasmonic sensing methods could be appealed for medical
508 applications such as in situ active nanorheology for viscosity measurements of complex biological
509 fluids, such as blood plasma.[84]

510

511 6. Conclusions and Perspectives

512 This review provides an overview of important methods for chiral sensing via chiroptical
513 spectroscopy as well as addresses possible mechanisms for chiral design that leads to generation and
514 amplification of the chiroptical response. Such chiral design and sensing applications are becoming
515 increasingly important in all areas of chemistry, biochemistry, and structural biology, including
516 implementing chiral systems of various scales and phases of mater, prominently in the arena of
517 pharmaceutical, agricultural, and optoelectronic industries. When different sources of chirality, such
518 as individual, collective and/or induced chirality are present in a molecular system, it may not be
519 possible to perform the structural analysis from an individual type of chiroptical response. Mindful
520 of the scope of applicability, merits and limitations of a given chiroptical method can be identified

521 when multiple methods are applied simultaneously to cross-examine a given stereochemical
522 structural objective. Some pharmaceutical companies have established a facility often termed as
523 “Chiral Tool Box” which contains chiroptical spectroscopic equipment and related computational
524 methods for analyzing the chiroptical responses. Particularly promising for advances in medicinal
525 fields are novel case studies, presented herein, which demonstrate chiral design and sensing as the
526 frontier in chiroptical diagnosis. We hope that this review will provide a source of inspiration for
527 novel types of chiral design and amplification mechanisms for current practitioners as well as a
528 valuable reference for future generation scientists.

529

530 **Funding:** This research was funded by Xunta de Galicia (ED431F 2016/005, GRC2019/24), IBEROS
531 (0245_IBEROS_1_E), and Slovenian Research Agency (ARRS) P4-0121”

532 **Acknowledgments:** A.O. thanks Xunta de Galicia for a predoctoral fellowship. J.L.A.-G. thanks the Spanish
533 Ministerio de Economía y Competividad for a “Ramón y Cajal” research contract.

534 **Conflicts of Interest:** The authors declare no conflict of interest.

535 References

- 536 1. Riehl, J.P. *Mirror-Image Asymmetry: An Introduction to the Origin and Consequences of Chirality*; 2010;
537 ISBN 9780470387597.
- 538 2. *Structure Elucidation in Organic Chemistry: The Search for the Right Tools*; Cid, M.M., Bravo, J., Eds.; 2015;
539 ISBN 9783527664610.
- 540 3. Gal, J. Louis Pasteur, language, and molecular chirality. I. Background and dissymmetry. *Chirality*
541 **2011**, *23*, 1–16.
- 542 4. Stephens, T.D.; Bunde, C.J.; Fillmore, B.J. Mechanism of action in thalidomide teratogenesis. *Biochem.*
543 *Pharmacol.* **2000**, *59*, 1489–1499.
- 544 5. Bentley, K.W.; Wolf, C. Comprehensive Chirality Sensing: Development of Stereodynamic Probes with
545 a Dual (Chir)optical Response. *J. Org. Chem.* **2014**, *79*, 6517–6531.
- 546 6. Polavarapu, P.L. Why is it important to simultaneously use more than one chiroptical spectroscopic
547 method for determining the structures of chiral molecules? *Chirality* **2008**, *20*, 664–672.
- 548 7. Polavarapu, P.L. Molecular structure determination using chiroptical spectroscopy: Where we may go
549 wrong? *Chirality* **2012**, *24*, 909–920.
- 550 8. Berova, N.; Polavarapu, P.L.; Nakanishi, K.; Woody, R.W. *Comprehensive Chiroptical Spectroscopy:*
551 *Instrumentation, Methodologies, and Theoretical Simulations, Volume 1*; 2012; ISBN 9781118120187.
- 552 9. Lassen, P.R.; Skytte, D.M.; Hemmingsen, L.; Nielsen, S.F.; Freedman, T.B.; Nafie, L.A.; Christensen, S.B.
553 Structure and absolute configuration of nyasol and hinokiresinol via synthesis and vibrational circular
554 dichroism spectroscopy. *J. Nat. Prod.* **2005**, *68*, 1603–1609.
- 555 10. G. Petrovic, A.; Alonso-Gomez, J.L.; Navarro-Vazquez, A. From Relative to Absolute Configuration of

- 556 Complex Natural Products: Interplay Between NMR, ECD, VCD, and ORD Assisted by ab initio
557 Calculations. *Curr. Org. Chem.* **2010**, *14*, 1612–1628.
- 558 11. Wang, Z.; Cheng, F.; Winsor, T.; Liu, Y. Optical chiral metamaterials: A review of the fundamentals,
559 fabrication methods and applications. *Nanotechnology* **2016**, *27*, 412001–412020.
- 560 12. Rivera-Fuentes, P.; Alonso-Gómez, J.L.; Petrovic, A.G.; Santoro, F.; Harada, N.; Berova, N.; Diederich,
561 F. Amplification of chirality in monodisperse, enantiopure alleno-acetylenic oligomers. *Angew. Chem.*
562 *Int. Ed. Engl.* **2010**, *49*, 2247–2250.
- 563 13. Fernández, B.; Rodríguez, R.; Quiñoá, E.; Riguera, R.; Freire, F. Decoding the ECD Spectra of
564 Poly(phenylacetylene): Structural Significance. *ACS Omega* **2019**, *4*, 5233–5240.
- 565 14. Castro-Fernández, S.; Yang, R.; García, A.P.; Garzón, I.L.; Xu, H.; Petrovic, A.G.; Alonso-Gómez, J.L.
566 Diverse Chiral Scaffolds from Diethynylspiranes: All-Carbon Double Helices and Flexible Shape-
567 Persistent Macrocycles. *Chem. Eur. J.* **2017**, *23*, 11747–11751.
- 568 15. Míguez-Lago, S.; Llamas-Saiz, A.L.; MagdalenaCid, M.; Alonso-Gómez, J.L. A Covalent Organic
569 Helical Cage with Remarkable Chiroptical Amplification. *Chem. - A Eur. J.* **2015**, *21*, 18085–18088.
- 570 16. Gidron, O.; Ebert, M.-O.; Trapp, N.; Diederich, F. Chiroptical detection of nonchromophoric, achiral
571 guests by enantiopure alleno-acetylenic helicages. *Angew Chem Int Ed.* **2014**, *53*, 13614–13618.
- 572 17. Guerrero-Martínez, A.; Alonso-Gómez, J.L.; Auguie, B.; Cid, M.M.; Liz-Marzán, L.M. From individual
573 to collective chirality in metal nanoparticles. *Nano Today* **2011**, *6*, 381–400.
- 574 18. Shao, K.; Lv, Z.; Xiong, Y.; Li, G.; Wang, D.; Zhang, H.; Qing, G. Circularly polarized light modulated
575 supramolecular self-assembly for an azobenzene-based chiral gel. *RSC Adv.* **2019**, *9*, 10360–10363.
- 576 19. Cheng, J.; Le Saux, G.; Gao, J.; Buffeteau, T.; Battie, Y.; Barois, P.; Ponsinet, V.; Delville, M.-H.H.; Ersen,
577 O.; Pouget, E.; et al. GoldHelix: Gold Nanoparticles Forming 3D Helical Superstructures with
578 Controlled Morphology and Strong Chiroptical Property. *ACS Nano* **2017**, *11*, 3806–3818.
- 579 20. Valderrey, V.; Aragay, G.; Ballester, P. Foldamers: A Manifesto. *Coord. Chem. Rev.* **2014**, *258–259*, 173–
580 156.
- 581 21. Li, C.Z.; Jiang, X.K.; Li, Z.T.; Gao, X.; Wang, Q.R. Foldamer-based molecular recognition. *Chinese J. Org.*
582 *Chem.* **2007**, *27*, 188–196.
- 583 22. Ferrand, Y.; Kendhale, A.M.; Kauffmann, B.; Grélard, A.; Marie, C.; Blot, V.; Pipelier, M.; Dubreuil, D.;
584 Huc, I. Diastereoselective encapsulation of tartaric acid by a helical aromatic oligoamide. *J. Am. Chem.*
585 *Soc.* **2010**, *132*, 7858–7859.
- 586 23. Valderrey, V.; Aragay, G.; Ballester, P. Porphyrin tweezer receptors: Binding studies, conformational
587 properties and applications. *Coord. Chem. Rev.* **2014**, *258–259*, 137–156.
- 588 24. Berova, N.; Pescitelli, G.; Petrovic, A.G.; Proni, G. Probing molecular chirality by CD-sensitive dimeric

- 589 metalloporphyrin hosts. *Chem. Commun.* **2009**, 5958–5980.
- 590 25. Míguez-Lago, S.; Cid, M.M.M.; Alonso-Gómez, J.L.; Míguez-Lago, S.; Cid, M.M.M.; Alonso-Gómez, J.L.
591 Covalent Organic Helical Cages as Sandwich Compound Containers. *European J. Org. Chem.* **2016**,
592 5716–5721.
- 593 26. Ajayaghosh, A.; Varghese, R.; Mahesh, S.; Praveen, V.K. From vesicles to helical nanotubes: A
594 sergeant-and-soldiers effect in the self-assembly of oligo(p-phenyleneethynylene)s. *Angew Chem Int Ed.*
595 **2006**, *45*, 7729–7732.
- 596 27. Pal, D.S.; Kar, H.; Ghosh, S. Controllable supramolecular polymerization: Via a chain-growth
597 mechanism. *Chem. Commun.* **2018**, *54*, 928–931.
- 598 28. Wen, T.; Shen, H.Y.; Wang, H.F.; Mao, Y.C.; Chuang, W.T.; Tsai, J.C.; Ho, R.M. Controlled Handedness
599 of Twisted Lamellae in Banded Spherulites of Isotactic Poly(2-vinylpyridine) as Induced by Chiral
600 Dopants. *Angew Chem Int Ed.* **2015**, *54*, 14313–14316.
- 601 29. Suárez-Picado, E.; Quiñoá, E.; Riguera, R.; Freire, F. Poly(phenylacetylene) Amines: A General Route to
602 Water-Soluble Helical Polyamines. *Chem. Mater.* **2018**, *30*, 6908–6914.
- 603 30. Pescitelli, G.; Di Bari, L. Revision of the Absolute Configuration of Preussilides A-F Established by the
604 Exciton Chirality Method. *J. Nat. Prod.* **2017**, *80*, 2855–2859.
- 605 31. Asai, T.; Taniguchi, T.; Yamamoto, T.; Monde, K.; Oshima, Y. Structures of spiroindicumides A and B,
606 unprecedented carbon skeletal spiro lactones, and determination of the absolute configuration by
607 vibrational circular dichroism exciton approach. *Org. Lett.* **2013**, *15*, 4320–4323.
- 608 32. Covington, C.L.; Nicu, V.P.; Polavarapu, P.L. Determination of the Absolute Configurations Using
609 Exciton Chirality Method for Vibrational Circular Dichroism: Right Answers for the Wrong Reasons? *J.*
610 *Phys. Chem. A* **2015**, *119*, 10589–10601.
- 611 33. Noumeur, S.R.; Helaly, S.E.; Jansen, R.; Gereke, M.; Stradal, T.E.B.; Harzallah, D.; Stadler, M.
612 Preussilides A-F, Bicyclic Polyketides from the Endophytic Fungus *Preussia similis* with
613 Antiproliferative Activity. *J. Nat. Prod.* **2017**, *80*, 1531–1540.
- 614 34. Pecul, M.; Ruud, K. The Ab Initio Calculation of Optical Rotation and Electronic Circular Dichroism.
615 *Adv. Quantum Chem.* **2005**, *50*, 185–212.
- 616 35. Crawford, T.D. Ab initio calculation of molecular chiroptical properties. *Theor. Chem. Acc.* **2006**, *115*,
617 227–245.
- 618 36. Polavarapu, P.L. Renaissance in chiroptical spectroscopic methods for molecular structure
619 determination. *Chem. Rec.* **2007**, *7*, 125–136.
- 620 37. Autschbach, J. Computing chiroptical properties with first-principles theoretical methods: Background
621 and illustrative examples. *Chirality* **2009**, *21*, E116–E152.

- 622 38. Pescitelli, G.; Bruhn, T. Good Computational Practice in the Assignment of Absolute Configurations by
623 TDDFT Calculations of ECD Spectra. *Chirality* **2016**, *28*, 466–474.
- 624 39. Zuber, G.; Goldsmith, M.R.; Hopkins, T.D.; Beratan, D.N.; Wipf, P. Systematic assignment of the
625 configuration of flexible natural products by spectroscopic and computational methods: The
626 bistramide C analysis. *Org. Lett.* **2005**, *7*, 5269–5272.
- 627 40. Johnson, J.L.; Raghavan, V.; Cimmino, A.; Moeini, A.; Petrovic, A.G.; Santoro, E.; Superchi, S.; Berova,
628 N.; Evidente, A.; Polavarapu, P.L. Absolute configurations of chiral molecules with multiple
629 stereogenic centers without prior knowledge of the relative configurations: A case study of inuloxin C.
630 *Chirality* **2018**, *30*, 1206–1214.
- 631 41. Brémond, E.; Savarese, M.; Adamo, C.; Jacquemin, D. Accuracy of TD-DFT Geometries: A Fresh Look.
632 *J. Chem. Theory Comput.* **2018**, *14*, 3715–3727.
- 633 42. Berardozi, R.; Guido, C.A.; Capozzi, M.A.M.; Cardellicchio, C.; Di Bari, L.; Pescitelli, G. Circular
634 Dichroism and TDDFT Investigation of Chiral Fluorinated Aryl Benzyl Sulfoxides. *European J. Org.*
635 *Chem.* **2015**, 5554–5562.
- 636 43. Bruhn, T.; Witterauf, F.; Götz, D.C.G.; Grimmer, C.T.; Würtemberger, M.; Radius, U.; Bringmann, G.
637 C,C- and N,C-coupled dimers of 2-aminotetraphenylporphyrins: Regiocontrolled synthesis,
638 spectroscopic properties, and quantum-chemical calculations. *Chem. - A Eur. J.* **2014**, *20*, 3998–4006.
- 639 44. Guennic, B. Le; Hieringer, W.; Görling, A.; Autschbach, J. Density functional calculation of the
640 electronic circular dichroism spectra of the transition metal complexes $[M(\text{phen})_3]^{2+}$ (M = Fe, Ru, Os).
641 *J. Phys. Chem. A* **2005**, *109*, 4836–4846.
- 642 45. Brémond, É.; Savarese, M.; Su, N.Q.; Pérez-Jiménez, Á.J.; Xu, X.; Sancho-García, J.C.; Adamo, C.
643 Benchmarking Density Functionals on Structural Parameters of Small-/Medium-Sized Organic
644 Molecules. *J. Chem. Theory Comput.* **2016**, *12*, 459–465.
- 645 46. Howard, J.C.; Sowndarya, S. V.; Ansari, I.M.; Mach, T.J.; Baranowska-ŁAczkowska, A.; Crawford, T.D.
646 Performance of Property-Optimized Basis Sets for Optical Rotation with Coupled Cluster Theory. *J.*
647 *Phys. Chem. A* **2018**, *122*, 5962–5969.
- 648 47. Mazzeo, G.; Giorgio, E.; Zanasi, R.; Berova, N.; Rosini, C. Absolute configuration through the DFT
649 simulation of the optical rotation. Importance of the correct selection of the input geometry: A caveat.
650 *J. Org. Chem.* **2010**, *75*, 4600–4603.
- 651 48. Mennucci, B.; Cappelli, C.; Cammi, R.; Tomasi, J. Modeling solvent effects on chiroptical properties.
652 *Chirality* **2011**, *23*, 717–729.
- 653 49. Petrovic, A.G.; Vantomme, G.; Negrón-Abril, Y.L.; Lubian, E.; Saielli, G.; Menegazzo, I.; Cordero, R.;
654 Proni, G.; Nakanishi, K.; Carofiglio, T.; et al. Bulky melamine-based Zn-porphyrin tweezer as a CD
655 probe of molecular chirality. *Chirality* **2011**, *23*, 808–19.

- 656 50. Troche-Pesqueira, E.; Pérez-Juste, I.; Navarro-Vázquez, A.; Cid, M.M. A β -cyclodextrin-resveratrol
657 inclusion complex and the role of geometrical and electronic effects on its electronic induced circular
658 dichroism. *RSC Adv.* **2013**, *3*, 10242–10250.
- 659 51. Giner-Casares, J.J.; Liz-Marzán, L.M. Plasmonic nanoparticles in 2D for biological applications: Toward
660 active multipurpose platforms. *Nano Today* **2014**, *9*, 365–377.
- 661 52. Tang, L.; Li, S.; Xu, L.; Ma, W.; Kuang, H.; Wang, L.; Xu, C. Chirality-based Au@Ag Nanorod Dimers
662 Sensor for Ultrasensitive PSA Detection. *ACS Appl. Mater. Interfaces* **2015**, *7*, 12708–12712.
- 663 53. Perera, A.S.; Thomas, J.; Poopari, M.R.; Xu, Y. The clusters-in-a-liquid approach for solvation: New
664 insights from the conformer specific gas phase spectroscopy and vibrational optical activity
665 spectroscopy. *Front. Chem.* **2016**, *4*, 1–17.
- 666 54. Lipparini, F.; Egidi, F.; Cappelli, C.; Barone, V. The optical rotation of methyloxirane in aqueous
667 solution: A never ending story? *J. Chem. Theory Comput.* **2013**, *9*, 1880–1884.
- 668 55. Kumar, J.; Eraña, H.; López-Martínez, E.; Claes, N.; Martín, V.F.; Solís, D.M.; Bals, S.; Cortajarena, A.L.;
669 Castilla, J.; Liz-Marzán, L.M. Detection of amyloid fibrils in Parkinson's disease using plasmonic
670 chirality. *Proc. Natl. Acad. Sci. U. S. A.* **2018**, *115*, 3225–3230.
- 671 56. Guerrero-Martínez, A.; Auguie, B.; Alonso-Gómez, J.L.; Džolič, Z.; Gómez-Graña, S.; Žinić, M.; Cid,
672 M.M.; Liz-Marzán, L.M. Intense optical activity from three-dimensional chiral ordering of plasmonic
673 nanoantennas. *Angew Chem Int Ed.* **2011**, *50*, 5499–5503.
- 674 57. Covington, C.L.; Polavarapu, P.L. Similarity in dissymmetry factor spectra: A quantitative measure of
675 comparison between experimental and predicted vibrational circular dichroism. *J. Phys. Chem. A* **2013**,
676 *117*, 3377–3386.
- 677 58. Junior, F.M.S.; Covington, C.L.; De Amorim, M.B.; Velozo, L.S.M.; Kaplan, M.A.C.; Polavarapu, P.L.
678 Absolute configuration of a rare sesquiterpene: (+)-3-ishwarone. *J. Nat. Prod.* **2014**, *77*, 1881–1886.
- 679 59. Johnson, J.L.; Sadasivan Nair, D.; Muraleedharan Pillai, S.; Johnson, D.; Kallingathodi, Z.; Ibnusaud, I.;
680 Polavarapu, P.L. Dissymmetry Factor Spectral Analysis Can Provide Useful Diastereomer
681 Discrimination: Chiral Molecular Structure of an Analogue of (–)-Crispine A. *ACS Omega* **2019**, *4*, 6154–
682 6164.
- 683 60. Harada, N.; Nakanishi, K. Exciton chirality method and its application to configurational and
684 conformational studies of natural products. *Acc. Chem. Res.* **1972**, *5*, 257–263.
- 685 61. Berova, N.; Di Bari, L.; Pescitelli, G.; Bari, L. Di; Pescitelli, G. Application of electronic circular
686 dichroism in configurational and conformational analysis of organic compounds. *Chem. Soc. Rev.* **2007**,
687 *36*, 914–931.
- 688 62. Castro-Fernández, S.; Peña-Gallego, Á.; Mosquera, R.A.; Alonso-Gómez, J.L. Chiroptical symmetry
689 analysis: Exciton chirality-based formulae to understand the chiroptical responses of C_n and D_n

- 690 symmetric systems. *Molecules* **2019**, *24*, 141–157.
- 691 63. Ozcelik, A.; Pereira-Cameselle, R.; Mosquera, R.A.; Peña-Gallego, Á.; Alonso-Gómez, J.L. Chiroptical
692 Symmetry Analysis of Trianglimines: A Case Study. *Symmetry (Basel)*. **2019**, *11*, 1245–1255.
- 693 64. Hentschel, M.; Schäferling, M.; Duan, X.; Giessen, H.; Liu, N. Chiral plasmonics. *Sci. Adv.* **2017**, *3*,
694 e1602735–e1602746.
- 695 65. Walters, R.S.; Kraml, C.M.; Byrne, N.; Ho, D.M.; Qin, Q.; Coughlin, F.J.; Bernhard, S.; Pascal, R.A.
696 Configurationally stable longitudinally twisted polycyclic aromatic compounds. *J. Am. Chem. Soc.* **2008**,
697 *130*, 16435–16441.
- 698 66. Alonso-Gómez, J.L.; Rivera-Fuentes, P.; Harada, N.; Berova, N.; Diederich, F. An enantiomerically pure
699 alleno-acetylenic macrocycle: Synthesis and rationalization of its outstanding chiroptical response.
700 *Angew Chem Int Ed.* **2009**, *48*, 5545–5548.
- 701 67. Pearlstein, R.M.; Davis, R.C.; Ditson, S.L. Giant circular dichroism of high molecular weight. *Proc Natl*
702 *Acad Sci U S A* **1982**, *79*, 400–402.
- 703 68. Lieberman, I.; Shemer, G.; Fried, T.; Kosower, E.M.; Markovich, G. Plasmon-resonance-enhanced
704 absorption and circular dichroism. *Angew. Chem. Int. Ed. Engl.* **2008**, *47*, 4855–7.
- 705 69. Guerrero-Martínez, A.; Auguie, B.; Alonso-Gómez, J.L.J.L.; Džolić, Z.; Gómez-Graña, S.; Žinić, M.; Cid,
706 M.M.M.; Liz-Marzán, L.M.L.M.; Džolić, Z.; Gómez-Graña, S.; et al. Intense optical activity from three-
707 dimensional chiral ordering of plasmonic nanoantennas. *Angew Chem Int Ed.* **2011**, *50*, 5499–5503.
- 708 70. White, S.J.; Johnson, S.D.; Sellick, M.A.; Bronowska, A.; Stockley, P.G.; Wälti, C. The influence of two-
709 dimensional organization on peptide conformation. *Angew Chem Int Ed.* **2015**, *54*, 974–978.
- 710 71. Zhang, Y.-Q.; Oner, M.A.; Lahoz, I.R.; Cirera, B.; Palma, C.-A.; Castro-Fernández, S.; Míguez-Lago, S.;
711 Cid, M.M.M.; Barth, J.V.; Alonso-Gómez, J.L.; et al. Morphological self-assembly of enantiopure
712 allenes for upstanding chiral architectures at interfaces. *Chem. Commun.* **2014**, *50*, 15022–15025.
- 713 72. Ozcelik, A.; Pereira-Cameselle, R.; Von Weber, A.; Paszkiewicz, M.; Carlotti, M.; Paintner, T.; Zhang,
714 L.; Lin, T.; Zhang, Y.Q.; Barth, J. V.; et al. Device-Compatible Chiroptical Surfaces through Self-
715 Assembly of Enantiopure Allenes. *Langmuir* **2018**, *34*, 4548–4553.
- 716 73. Ariga, K.; Richards, G.J.; Ishihara, S.; Izawa, H.; Hill, J.P. Intelligent chiral sensing based on
717 supramolecular and interfacial concepts. *Sensors* **2010**, *10*, 6796–820.
- 718 74. Hendry, E.; Carpy, T.; Johnston, J.; Popland, M.; Mikhaylovskiy, R. V.; Laphorn, A.J.; Kelly, S.M.;
719 Barron, L.D.; Gadegaard, N.; Kadodwala, M. Ultrasensitive detection and characterization of
720 biomolecules using superchiral fields. *Nat. Nanotechnol.* **2010**, *5*, 783–787.
- 721 75. Kelly, C.; Tullius, R.; Laphorn, A.J.; Gadegaard, N.; Cooke, G.; Barron, L.D.; Karimullah, A.S.; Rotello,
722 V.M.; Kadodwala, M. Chiral Plasmonic Fields Probe Structural Order of Biointerfaces. *J. Am. Chem. Soc.*

- 723 2018, *140*, 8509–8517.
- 724 76. Tullius, R.; Platt, G.W.; Khosravi Khorashad, L.; Gadegaard, N.; Lapthorn, A.J.; Rotello, V.M.; Cooke,
725 G.; Barron, L.D.; Govorov, A.O.; Karimullah, A.S.; et al. Superchiral Plasmonic Phase Sensitivity for
726 Fingerprinting of Protein Interface Structure. *ACS Nano* **2017**, *11*, 12049–12056.
- 727 77. Schäferling, M.; Dregely, D.; Hentschel, M.; Giessen, H. Tailoring Enhanced Optical Chirality: Design
728 Principles for Chiral Plasmonic Nanostructures. *Phys. Rev. X* **2012**, *2*, 031010–031019.
- 729 78. Zhao, Y.; Askarpour, A.N.; Sun, L.; Shi, J.; Li, X.; Alù, A. Chirality detection of enantiomers using
730 twisted optical metamaterials. *Nat. Commun.* **2017**, *8*, 14180–14188.
- 731 79. Yoo, S.; P.; Q-Han Metamaterials and chiral sensing: a review of fundamentals and applications.
732 *Nanophotonics* **2019**, *8*, 249–261.
- 733 80. Grimsdale, A.C.; Müllen, K. The chemistry of organic nanomaterials. *Angew Chem Int Ed.* **2005**, *44*,
734 5592–5629.
- 735 81. Monti, D.; Nardis, S.; Stefanelli, M.; Paolesse, R.; Di Natale, C.; D'Amico, A. Porphyrin-based
736 nanostructures for sensing applications. *J. Sensors* **2009**, *2009*, 1-10.
- 737 82. Stefanelli, M.; Magna, G.; Zurlo, F.; Caso, F.M.; Di Bartolomeo, E.; Antonaroli, S.; Venanzi, M.;
738 Paolesse, R.; Di Natale, C.; Monti, D. Chiral Selectivity of Porphyrin-ZnO Nanoparticle Conjugates.
739 *ACS Appl. Mater. Interfaces* **2019**, *11*, 12077–12087.
- 740 83. Šť'ováčková, L.; Tatarkovič, M.; Logerová, H.; Vavřinec, J.; Setnička, V. Identification of spectral
741 biomarkers for type 1 diabetes mellitus using the combination of chiroptical and vibrational
742 spectroscopy. *Analyst* **2015**, *140*, 2266–2272.
- 743 84. Jeong, H.-H.; Mark, A.G.; Lee, T.-C.; Alarcn-Correa, M.; Eslami, S.; Qiu, T.; Gibbs, J.G.; Fischer, P.
744 Active Nanorheology with Plasmonics. *Nano Lett.* **2016**, *16*, 4887–4894.